Biochemical and Biophysical Research Communications 405 (2011) 91–95

Contents lists available at ScienceDirect

Biochemical and Biophysical Research Communications

journal homepage: www.elsevier.com/locate/ybbrc

$A\beta_{40}$(L17A/F19A) mutant diminishes the aggregation and neurotoxicity of $A\beta_{40}$

Yi-Ru Chen [a,b,1], Hsien-bin Huang [c,1], Chi-Jen Lo [a,d,e], Chih-Ching Wang [a,d], Chia-Li Su [c], Hsin-Tzu Liu [f], Ming-Shi Shiao [g], Ta-Hsien Lin [a,d,e,*], Yi-Chen Chen [h,*]

[a] Structural Biology Program, National Yang-Ming University, Taipei 112, Taiwan, ROC
[b] Department and Institute of Pharmacology, National Yang-Ming University, Taipei 112, Taiwan, ROC
[c] Department of Life Science and Institute of Molecular Biology, National Chung Cheng University, Chia-Yi 621, Taiwan, ROC
[d] Department of Medical Research & Education, Taipei Veterans General Hospital, Taipei 112, Taiwan, ROC
[e] Institute of Biochemistry and Molecular Biology, National Yang-Ming University, Taipei 112, Taiwan, ROC
[f] Voiding Dysfunction Therapeutic Center in Research Department, Buddhist Tzu Chi General Hospital, Hualien 970, Taiwan
[g] Department of Life Science, Chang Gung University, Kwei-Shan Tao-Yuan 333, Taiwan, ROC
[h] Department of Medicine, Mackay Medical College, Taipei county 252, Taiwan, ROC

ARTICLE INFO

Article history:
Received 16 December 2010
Available online 7 January 2011

Keywords:
NMR
Thioflavin-T
β-amyloid peptide
Alzheimer's disease

ABSTRACT

Aggregated β-amyloid peptides (Aβ) are neurotoxic and responsible for neuronal death both *in vitro* and *in vivo*. From the structural point of view, Aβ self-aggregation involves a conformational change in the peptide. Here, we investigated the relationship between conformational changes and amino acid residues of $A\beta_{40}$. Urea unfolding in combination with NMR spectroscopy was applied to probe the stabilization of $A\beta_{40}$ conformation. L17 and F19 residues were found more sensitive to environmental changes than the other residues. Replacement of these two residues with alanine could stabilize the conformation of $A\beta_{40}$. Further analysis indicated that the $A\beta_{40}$(L17A/F19A) mutant could diminish the aggregation and reduce the neurotoxicity. These results suggest that L17 and F19 are the critical residues responsible for conformational changes which may trigger neurotoxic cascade of $A\beta_{40}$.

1. Introduction

Alzheimer's disease (AD) is the most common form of neurodegenerative disease [1]. The most important pathological hallmark is the amyloid senile plaques (SPs). The main component of SPs is a small and hydrophobic peptide-amyloid β (Aβ) which is derived from a ubiquitous type I transmembrane protein – amyloid precursor protein (APP) and spans residues 1–40 ($A\beta_{40}$) or 1–42 ($A\beta_{42}$) [2] The aggregation of Aβ has been demonstrated to play an early and essential role in the neuronal degeneration [1]. The generation of Aβ from APP involves a two-step cleavage process, an initial proteolysis by an aspartyl protease – β-secretase, and then cleavage by an intramembrane aspartic protease – β-secretase, to release Aβ [3,4]. The aggregates of Aβ, including oligomer, protofibril and fibril, have been shown to be the main toxic agents that lead to neurodegeneration and dementia [3,5,6].

The aggregation and toxicity of Aβ is highly correlated with its sequence and structure [7–10]. The effect of Aβ sequence on aggregation and toxicity has been studied using different Aβ fragments or truncated Aβ peptides [8,9]. In general, residues 17–21, 30–35 and 41–42 are the most important regions for aggregation and neurotoxicity. The conformation of Aβ undergoes a structural conversion from either α-helix or random coil to β-sheet during aggregation process, suggesting that conformational change is a key step in Aβ-aggregation cascade [8,10]. Study of the effect of amino acid residues on the conformational change of Aβ may provide useful information for further understanding the molecular mechanism of Aβ aggregation.

Previous studies have demonstrated that the Aβ aggregation can be blocked by the helix inducing reagents, such as trifluoroethanol (TFE) and sodium dodecyl sulfate (SDS) [11,12], and many efforts hence have been put to elucidate the contribution of amino acid residues on helix stabilization[10,13,14]. Based on this assumption, in this study, we applied a combination of urea denaturation and NMR spectroscopy to probe the conformation stability of $A\beta_{40}$ under helix-inducing reagent, SDS. Unlike other studies [10,13,14], the use of urea folding and NMR spectroscopy can allow us to have a full spectrum to inspect the contribution of amino acid residues on the stabilization of $A\beta_{40}$ conformation at single-residue resolution. Our result suggests that all of the residues in the α-helical region remain α-helical at 4 M urea except residues L17

Abbreviations: Aβ, β-amyloid peptide; AD, Alzheimer's disease; CD, circular dichroism; ThT, Thioflavin-T; SDS, sodium dodecyl sulfate.

* Corresponding authors Address: Department of Medicine, Mackay Medical College, Taipei county 252, Taiwan, ROC (Yi-Chen Chen). Department of Medical Research & Education, Taipei Veterans General Hospital, Taipei 112, Taiwan, ROC. Fax: +886 2 8751562 (Ta-Hsien Lin).

E-mail addresses: thlin@vghtpe.gov.tw (T.-H. Lin), chen15@mmc.edu.tw (Y.-C. Chen).

[1] These authors contributed equally to this work.

0006-291X/$ - see front matter © 2011 Elsevier Inc. All rights reserved.
doi:10.1016/j.bbrc.2010.12.133

and F19. We further mutated the L17 and F19 with alanine to study the structural stability of $A\beta_{40}$. The result showed that replacement of L17 and F19 with alanine can inhibit the conformational changes of $A\beta_{40}$ and that the mutation significantly reduces the aggregative ability and neurotoxicity of $A\beta_{40}$.

2. Material and methods

2.1. Synthesis of Aβ peptide

The synthesis of unlabeled wild-type $A\beta_{40}$ and mutated $A\beta_{40}$(17A/19A) peptides was performed using a solid-phase peptide synthesizer (ABI 433A) following the standard protocol. For NMR spectroscopic study, stable isotope labeled (either ^{15}N-labeled or ^{15}N, ^{13}C-labeled) $A\beta_{40}$ were synthesized using a cloning protocol as described elsewhere [7]. Both unlabeled and labeled Aβ peptides were purified on a reverse-phase C-18 HPLC with a linear gradient from 0% to 100% acetonitrile. The molecular weights of Aβ peptides were verified by MALDI-TOF mass spectroscopy.

2.2. NMR spectroscopy

For NMR experiments, either ^{15}N- or ^{15}N, ^{13}C-labeled $A\beta_{40}$ sample was dissolved in 100% TFE and dried under N_2 gas. Then this sample was redissolved in 0.25 ml 10 mM phosphate buffer, pH 6.0, 100 mM sodium dodecyl sulfate (SDS-d_{25}), 0.02% sodium azide, 10% (v/v) D_2O/H_2O with 0, 1, 2, 3, 4, and 5 M urea, respectively, to make a final $A\beta_{40}$ concentration of ~0.5 mM. The final protein sample solutions were transferred to 5 mm Shigemi NMR tubes (Shigemi Co.) for recording NMR spectra. NMR experiments were performed at 296 K on Bruker AVANCE-500 spectrometer equipped with a 5 mm inverse triple resonance ($^1H/^{13}C$/BB), Z-axis gradient probe or AVANCE-600 spectrometer equipped with a 5 mm inverse triple resonance ($^1H/^{13}C/^{15}N$), XYZ-axis gradient probe. All spectra were processed using the program TopSpin and analyzed using AURELIA (Bruker). Linear prediction was used in the indirectly detected dimensions to improve the digital resolution. Backbone sequential assignments were accomplished by using the following heteronuclear 3D spectra: HNCO, HN(CA)CO, HNCA, HN(CO)CA, CBCANH, CBCA(CO)NH. A home-written Fortran program has been used to search the sequential connectivity semi-automatically.

2.3. Circular dichroism spectroscopy and secondary structure analyses

For CD measurements, a final Aβ peptide concentration of 75 μM in 10 mM phosphate buffer, pH 7.0, was used. CD spectra were recorded using an Aviv410 spectropolarimeter equipped with a thermal circulator accessory. All measurements were performed in quartz cells with a pathlength of 0.1 cm. Data were collected at wavelengths from 190 to 260 nm in 0.2 nm increments. Every CD spectrum is reported as the average from at least three individual samples. The reported CD spectra were corrected for baseline using the phosphate buffer, pH 7.4. All measurements were carried out at 25.0 ± 0.2 °C. Secondary structure analysis was performed in an online web sever: Dichroweb [15–17] using CDSSTR program.

2.4. Peptide aggregation assay

Thioflavin-T (ThT) was used to monitor the aggregation state of Aβ peptides [18]. Peptides were prepared as a 1 mM stock solution in TFE, dried under N_2 gas, and resuspended in 10 mM phosphate buffer, pH 7.0 to a final peptide concentration of 75 μM. The resulting solutions were dispended into 1.5 ml vials, and stored at −80 °C until used. In order to accelerate the aggregation process, all experiments were carried out at a final peptide concentration of 75 μM with 75 μM ThT and 0.01% NaN_3 at 37 °C. The fluorescence measurements were performed on the SpectraMax M5 multimode microplate reader at 37.0 ± 0.2 °C. The excitation and emission wavelengths were 450 and 482 nm, respectively.

2.5. Cell culture

The rat pheochromocytoma cell line (PC12) was obtained from the American Type Culture Collection (ATCC). The PC12 pheochromocytoma was cultured in Ham's F12K medium with 15% (v/v) horse serum, 2.5% fetal bovine serum, 2 mM glutamine and antibiotics at 37 °C in a humidified atmosphere containing 5% CO_2. The cell suspension was obtained by passing the culture through a 22-gauge needle three times. Cells were subcultured every 4 or 5 days with a split ratio of 1:3–2:3. PC12 cells were differentiated with 50 ng/ml NGF in Ham's F12K in the absence of serum.

2.6. Cell viability assay

The cell viability was measured using the WST-1 assay [19]. Both wild-type and $A\beta_{40}$(L17A/F19A) mutant were prepared as a 1 mM stock solution in DMSO. Fresh prepared stock solution was then dried under N_2 gas, and resuspended in PBS buffer, pH 7.0, to a final peptide concentration of 500 μM. The resulting solution was incubated at 25 °C for 24 h. This incubated peptide solution was further diluted to 30 μM for viability assay. In a 96-well microtiter plate, 5×10^5 cells were incubated in the absence or presence of Aβ peptides in a total volume of 100 μl per well for 48 h at 37 °C in a humidified atmosphere containing 5% CO_2 before the viability assay. The WST-1 solution (10 μl) was added to each well, and the wells were incubated for another 0.5–4 h at room temperature. The absorbance was measured at a wavelength of 450 nm using a microtiter plate reader.

3. Results

3.1. NMR study of $A\beta_{40}$ structure under urea titration

To investigate the relationship between conformational changes and amino acid residues of $A\beta_{40}$, our approach is firstly to probe the conformational stability for each amino acid residue by using equilibrium denaturation and NMR spectroscopy under α-helix-stable reagent, SDS. Fig. 1(A) shows the two-dimensional ^1H-^{15}N-HSQC spectra of ^{15}N-enriched $A\beta_{40}$ in SDS solution. All of the backbone amide proton and ^{15}N resonances were assigned, except of the missing N-terminal Asp1 residue. The $^{13}C^\alpha$ chemical shift of each residue of $A\beta_{40}$ was determined at different concentrations of urea. $^{13}C^\alpha$ chemical shifts are known to be sensitive to the backbone structure of a polypeptide chain and widely used as a measure of secondary structure of a polypeptide. The $^{13}C^\alpha$ secondary chemical shift used in the present study was calculated by subtracting the $^{13}C^\alpha$ chemical shift of each amino acid residue in a random coil conformation from the experimental value to evaluate the extent of the unfolding induced by urea. In principle, a residue is defined to adopt an α-helical conformation when its $^{13}C^\alpha$ secondary chemical shift is greater than 0.7 ppm, and defined to adopt a β-strand conformation when its $^{13}C^\alpha$ secondary chemical shift is less than −0.7 ppm. When $^{13}C^\alpha$ secondary chemical shift of a residue is between −0.7 and 0.7 ppm, it adopts a random coil conformation.

The plots of $^{13}C^\alpha$ secondary chemical shift as a function of residue number and a function of urea concentration are shown in Fig. 1(B) and (C), respectively. In SDS micelles and 0 M urea, $A\beta_{40}$ basically adopts two short α-helical structures at residues 15–26 and 28–34 and random coiled structure for the rest residues. The

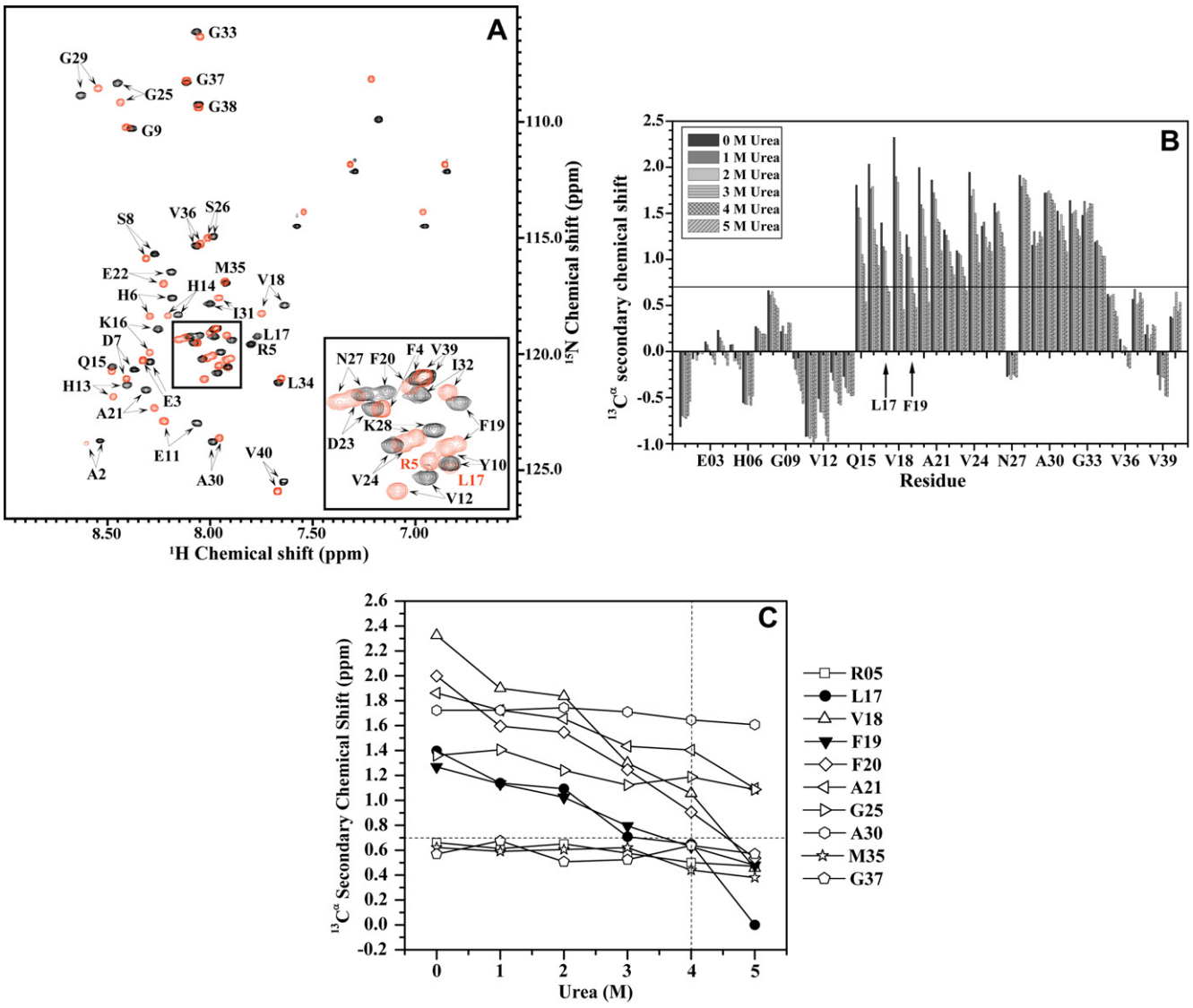

Fig. 1. (A) 2D ^{1}H-^{15}N-HSQC spectra of ^{15}N-enriched Aβ_{40} in 100 mM SDS-d_{25} solution at 0 (black) and 3 M (red) of urea. Assignments of the backbone amide protons and ^{15}N cross peaks are indicated in the figure. (B) The plot of $^{13}C^{\alpha}$ secondary chemical shift under 0–5 M urea vs. amino acid residue of Aβ_{40}. (C) The plot of representative $^{13}C^{\alpha}$ secondary chemical shift vs. urea concentration, (□) R05, (●) L17, (△) V18, (⬟) F19, (◇) F20, (◁) A21, (▷) G25, (○) G30, (☆) M35, (▽) G37. The horizontal and vertical lines indicate the $^{13}C^{\alpha}$ secondary chemical shift of 0.7 ppm and 4 M urea, respectively. It can be seen that the $^{13}C^{\alpha}$ secondary chemical shifts for L17 and F19 reduce under 0.7 ppm at 4 M, indicating that urea-induced unfolding of Aβ_{40} is more significant at these two residues.

structural feature is very similar to that obtain from proton NMR spectroscopy [20]. Upon urea titration, only a couple of residues in the first α-helix (residues 15–26) display significant $^{13}C^{\alpha}$ secondary chemical shift changes, while the $^{13}C^{\alpha}$ secondary chemical shifts of the residues in the second α-helix (residues 28–34) are slightly perturbed by urea. This result suggests that the second α-helix does not undergo structural change upon urea titration. As proposed by Gräslund et al. [21], the plausible reason for this phenomenon may be due to that the second α-helix might insert into the SDS micelles. After examining the data more closely, we found that the $^{13}C^{\alpha}$ secondary chemical shifts of residues L17 and F19 are very close to 0.7 ppm at 3 M urea. At 4 M urea, the $^{13}C^{\alpha}$ secondary chemical shifts of these two residues have reduced to less than 0.7 ppm, while the $^{13}C^{\alpha}$ secondary chemical shifts for the rest of the residues in the first α-helix remain over 0.7 ppm as depicted in Fig. 1(B). According to the relationship between helicity and $^{13}C^{\alpha}$ secondary chemical shift, our result suggests that all of the residues in the first α-helix remain α-helical at 4 M urea except residues L17 and F19. From the structural point of view, this result indicated that the extent of α-helix unfolding at residues L17 and F19 is more significant than that at the other residues in the α-helical region. The first α-helix is apt to unfold at residues L17 and F19 under urea titration, implying that these two residues are thermodynamically unfavorable for α-helix formation.

3.2. Mutational study on the conformational stability of Aβ_{40}

To further investigate the effect of residues 17 and 19 on the conformational stability of Aβ_{40} following the result obtained in NMR study, we performed mutational study of Aβ_{40}. Alanine has been thought to have a higher α-helical propensity. Replacement of these two residues with alanine may be able to increase the α-helical propensity of Aβ_{40}. Furthermore, it also has been showed that the alanine replacement of amino acid at residues 15–36 can destabilize the fibril elongation [10,16]. Therefore, we constructed a Aβ_{40}(L17A/F19A) mutant and applied circular dichroism (CD) spectroscopy to investigate the structural stability for the wild-type Aβ_{40} and Aβ_{40}(L17A/F19A). The CD spectra for Aβ_{40} and

$A\beta_{40}$(L17A/F19A) at various times are shown in Fig. 2(A) and (B), respectively. Further analysis of β-sheet propensity (CD signal at 218 nm vs. time) is shown in Fig. 2(C). The intensity of 218 nm is increased with an increase of time for $A\beta_{40}$, suggesting that the conformation of wild-type $A\beta_{40}$ is gradually converted into β-sheet structure. On the other hand, the intensity of 218 nm is kept at constant level for $A\beta_{40}$(L17A/F19A). It is apparent that wild-type $A\beta_{40}$ underwent a conformational conversion from random coil into β-sheet, while no conformational change could be observed for $A\beta_{40}$(L17A/F19A), and the conformation of $A\beta_{40}$(L17A/F19A) stably remained at random coiled state. The result of CD analysis suggests that the replacement of L17 and F19 with alanine can increase the conformational stability of $A\beta_{40}$.

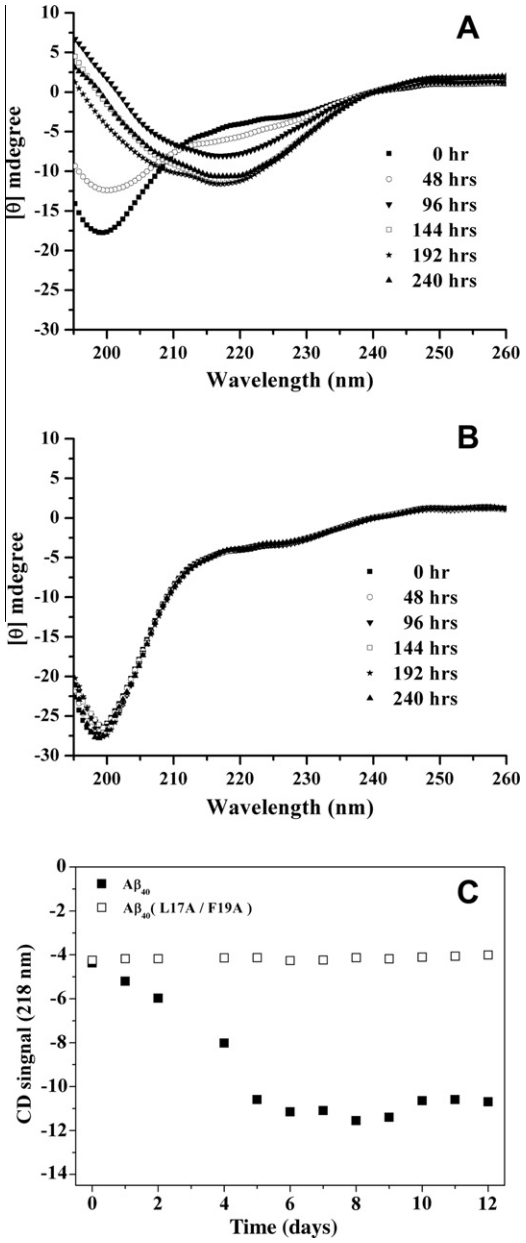

Fig. 2. Far ultraviolet circular dichroism spectra for (A) wild-type and (B) Aβ40(L17A/F19A) peptides at various incubated times. Aβ peptides were used at a concentration of 10 μM for CD measurement. (C) CD intensity at 218 nm as function of incubation time.

3.3. Aggregative ability of $A\beta_{40}$ and $A\beta_{40}$(L17A/F19A)

We also performed kinetic aggregation study to further confirm the effect of L17 and F19 on the aggregative ability of $A\beta_{40}$. Fig. 3 shows the aggregation process for $A\beta_{40}$ and $A\beta_{40}$(L17A/F19A) using ThT assay. It can be seen that the aggregation rate of wild-type $A\beta_{40}$ is obviously much faster than that of $A\beta_{40}$(L17A/F19A). Comparatively, at around 20 h, the aggregation of wild-type $A\beta_{40}$ reached a steady state, while the aggregation process of $A\beta_{40}$(L17A/F19A) remains at lag phase through the whole incubation period, suggesting that the aggregation ability of $A\beta_{40}$(L17A/F19A) is reduced compared to that of wild-type $A\beta_{40}$.

3.4. Cell viability assay

As shown in our present results, $A\beta_{40}$(L17A/F19A) reduces the ability of aggregation and does not undergo conformational change. In order to further compare the neurotoxicity between $A\beta_{40}$ and $A\beta_{40}$(L17A/F19A), the comparative cell viability of $A\beta_{40}$ and $A\beta_{40}$(L17A/F19A) was studied. Fig. 4 shows the comparative cell viability treated with 30 μM of $A\beta_{40}$ and $A\beta_{40}$(L17A/F19A) peptides 48 h. Obviously, the neurotoxicity induced by $A\beta_{40}$ was much stronger than that by $A\beta_{40}$(L17A/F19A). At treated with 30 μM of $A\beta_{40}$ and $A\beta_{40}$(L17A/F19A) 48 h, the related cell survival rates for $A\beta_{40}$ and $A\beta_{40}$(L17A/F19A) were around 36% and 85%, respectively. This suggests that $A\beta_{40}$(L17A/F19A) is also less toxic than $A\beta_{40}$.

4. Discussion

In the present study, we demonstrate that the combination of urea denaturation and NMR spectroscopic techniques can be successfully applied to study the relationship between conformational stability and sequence of $A\beta_{40}$. Previously, residues 16–23 have been predicted as the region of discordant helix [13], and any factors which stabilize the conformation of this discordant helix region can prevent the aggregation of $A\beta_{40}$. Our present study echoes with this hypothesis which results show that residues 17–20 are the most sensible region for the environmental changes and may play an important role on $A\beta_{40}$ conformational change.

Previously, Williams and colleagues have concluded that any single alanine mutation of $A\beta_{40}$ will cause the difference on structural stability but won't inhibit the aggregation [14]. A similar mutation study was obtained by Paivio et al., which based on an *in silicon* prediction [10], the ability of $A\beta_{40}$ fibril formation was reduced by introducing V18A/F19A/F20A replacement.

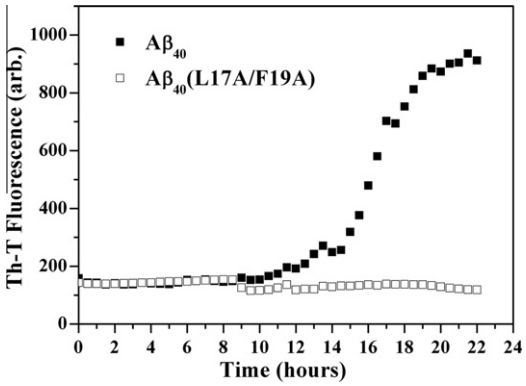

Fig. 3. Aggregation process of wild-type $A\beta_{40}$ and Aβ40(L17A/F19A) peptides: $A\beta_{40}$(■) and $A\beta_{40}$(L17A/F19A) (□). The aggregation assay was performed with 75 μM of Aβ peptides, 75 μM Th-T and 0.01% NaN_3 at 37 °C.

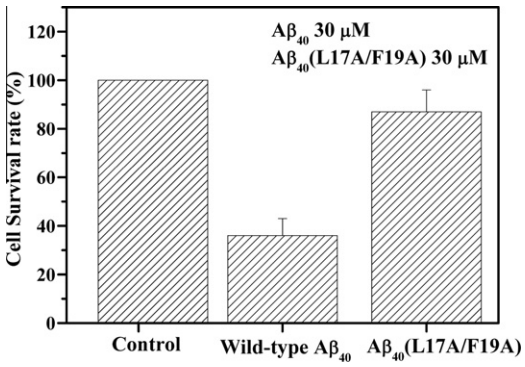

Fig. 4. Comparison of neurotoxicity of wild-type $A\beta_{40}$ and Aβ40(L17A/F19A) peptides. Aβ peptides at a final concentration of 30 μM were incubated with PC12 cells for 48 h. The percentage of cell viability was measured using the WST-1 assay. The wells containing PC12 cells without Aβ peptides were used as negative control.

However, by using urea denaturation and NMR spectroscopic techniques, we further indentified that among residues 17–20, the amino acids L17 and F19 may play a key role on the stabilization of $A\beta_{40}$ conformation. By constructing an $A\beta_{40}$(L17A/F19A) mutant and characterizing its conformational stability, aggregative ability, secondary structure and neurotoxicity, we showed that the $A\beta_{40}$(L17A/F19A) mutant adopts a random coiled structure and does not undergo any structural conversion. The neurotoxicity of $A\beta_{40}$(L17A/F19A) is also less toxic than that of wild-type $A\beta_{40}$. The comparative cell viability of $A\beta_{40}$(L17A/F19A) is almost 2.5-folds greater than that of $A\beta_{40}$. Therefore, our result indicates that instead of V18, F19 and F20, only L17 and F19 may be enough to stabilize the conformation of $A\beta_{40}$ and inhibit its aggregation.

In conclusion, our result reinforced that the discordant helix is most sensitive to environmental changes and may play a key role in stabilization of $A\beta_{40}$ conformation. Moreover, our study further demonstrates that residues L17 and F19 may play a critical role on the stabilization of $A\beta_{40}$ conformation. Instead of replacement of V18/F19/F20 into A18/A19/A20, the changes of structural nature of L17 and F19, such as alanine replacement of L17 and F19, may stabilize the conformation of $A\beta_{40}$, diminish the aggregation of $A\beta_{40}$ and reduce the neurotoxicity induced by $A\beta_{40}$ peptide.

Acknowledgments

This work was supported by grants from National Science Council of Taiwan, ROC (NSC 96-2311-B-010-010-MY3 to T. H. L. and NSC97-2627-M-715-001 to Y. C. C.) and Taipei Veterans General Hospital, Taiwan, Republic of China (V96C1-022, V96S4-002 to T. H. L.). The NMR spectra were obtained at High-Field Biomacromolecular NMR Core Facility supported by the National Research Program for Genomic Medicine.

References

[1] D.J. Selkoe, The molecular pathology of Alzheimer's disease, Neuron 6 (1991) 487–498.
[2] R.E. Tanzi, E.D. Bird, S.A. Latt, R.L. Neve, The amyloid beta protein gene is not duplicated in brains from patients with Alzheimer's disease, Science 238 (1987) 666–669.
[3] Y.M. Li, M. Xu, M.T. Lai, Q. Huang, J.L. Castro, J. DiMuzio-Mower, T. Harrison, C. Lellis, A. Nadin, J.G. Neduvelil, R.B. Register, M.K. Sardana, M.S. Shearman, A.L. Smith, X.P. Shi, K.C. Yin, J.A. Shafer, S.J. Gardell, Photoactivated gamma-secretase inhibitors directed to the active site covalently label presenilin 1, Nature 405 (2000) 689–694.
[4] R. Vassar, B.D. Bennett, S. Babu-Khan, S. Kahn, E.A. Mendiaz, P. Denis, D.B. Teplow, S. Ross, P. Amarante, R. Loeloff, Y. Luo, S. Fisher, J. Fuller, S. Edenson, J. Lile, M.A. Jarosinski, A.L. Biere, E. Curran, T. Burgess, J.C. Louis, F. Collins, J. Treanor, G. Rogers, M. Citron, Beta-secretase cleavage of Alzheimer's amyloid precursor protein by the transmembrane aspartic protease BACE, Science 286 (1999) 735–741.
[5] K.N. Dahlgren, A.M. Manelli, W.B. Stine Jr., L.K. Baker, G.A. Krafft, M.J. LaDu, Oligomeric and fibrillar species of amyloid-beta peptides differentially affect neuronal viability, J. Biol. Chem. 277 (2002) 32046–32053.
[6] D.J. Selkoe, T. Yamazaki, M. Citron, M.B. Podlisny, E.H. Koo, D.B. Teplow, C. Haass, The role of APP processing and trafficking pathways in the formation of amyloid beta-protein, Ann. NY Acad. Sci. 777 (1996) 57–64.
[7] E.K. Lee, J.H. Hwang, D.Y. Shin, D.I. Kim, Y.J. Yoo, Production of recombinant amyloid-beta peptide 42 as an ubiquitin extension, Protein Expr. Purif. 40 (2005) 183–189.
[8] M.Q. Liao, Y.J. Tzeng, L.Y. Chang, H.B. Huang, T.H. Lin, C.L. Chyan, Y.C. Chen, The correlation between neurotoxicity, aggregative ability and secondary structure studied by sequence truncated Abeta peptides, FEBS Lett. 581 (2007) 1161–1165.
[9] R. Liu, C. McAllister, Y. Lyubchenko, M.R. Sierks, Residues 17–20 and 30–35 of beta-amyloid play critical roles in aggregation, J. Neurosci. Res. 75 (2004) 162–171.
[10] A. Paivio, E. Nordling, Y. Kallberg, J. Thyberg, J. Johansson, Stabilization of discordant helices in amyloid fibril-forming proteins, Protein Sci. 13 (2004) 1251–1259.
[11] C.J. Barrow, K. Nakanishi, K. Tachibana, Structure and activity studies of pardaxin and analogues using model membranes of phosphatidylcholine, Biochim. Biophys. Acta 1112 (1992) 235–240.
[12] O. Crescenzi, S. Tomaselli, R. Guerrini, S. Salvadori, A.M. D'Ursi, P.A. Temussi, D. Picone, Solution structure of the Alzheimer amyloid beta-peptide (1–42) in an apolar microenvironment. Similarity with a virus fusion domain, Eur. J. Biochem. 269 (2002) 5642–5648.
[13] Y. Kallberg, M. Gustafsson, B. Persson, J. Thyberg, J. Johansson, Prediction of amyloid fibril-forming proteins, J. Biol. Chem. 276 (2001) 12945–12950.
[14] A.D. Williams, S. Shivaprasad, R. Wetzel, Alanine scanning mutagenesis of Abeta(1–40) amyloid fibril stability, J. Mol. Biol. 357 (2006) 1283–1294.
[15] L. Whitmore, B.A. Wallace, DICHROWEB, an online server for protein secondary structure analyses from circular dichroism spectroscopic data, Nucleic Acids Res. 32 (2004) 668–673.
[16] L.A. Compton, W.C. Johnson Jr., Analysis of protein circular dichroism spectra for secondary structure using a simple matrix multiplication, Anal. Biochem. 155 (1986) 155–167.
[17] A. Lobley, L. Whitmore, B.A. Wallace, DICHROWEB: an interactive website for the analysis of protein secondary structure from circular dichroism spectra, Bioinformatics 18 (2002) 211–212.
[18] P.H. Levine, A. Manns, Transfusion transmission of human T-lymphotropic virus types I and II: lessons to be learned from look-back investigations and implications for patient counseling, Transfusion 33 (1993) 4–6.
[19] M.B. Hansen, S.E. Nielsen, K. Berg, Re-examination and further development of a precise and rapid dye method for measuring cell growth/cell kill, J. Immunol. Methods 119 (1989) 203–210.
[20] M. Coles, W. Bicknell, A.A. Watson, D.P. Fairlie, D.J. Craik, Solution structure of amyloid beta-peptide(1–40) in a water-micelle environment. Is the membrane-spanning domain where we think it is?, Biochemistry 37 (1998) 11064–11077
[21] J. Jarvet, J. Danielsson, P. Damberg, M. Oleszczuk, A. Gräslund, Positioning of the Alzheimer Abeta(1–40) peptide in SDS micelles using NMR and paramagnetic probes, J Biomol NMR 39 (2007) 63–72.